Effect of receptor phosphorylation on the binding between IRS-1 and IGF-1R as revealed by surface plasmon resonance biosensor

Minghui Huang[a], Wan Ping Lai[b], Man Sau Wong[b,1], Mengsu Yang[a,*]

[a] *Applied Research Center for Genomic Technology, and Department of Biology and Chemistry, City University of Hong Kong, 83 Tat Chee Avenue, Kowloon, Hong Kong, PR China*

[b] *Open Laboratory of Asymmetric Synthesis, Department of Applied Biology and Chemical Technology, Hong Kong Polytechnic University, Kowloon, Hong Kong, PR China*

Received 18 June 2001; revised 18 July 2001; accepted 19 July 2001

First published online 14 August 2001

Edited by Gianni Cesareni

Abstract A receptor binding assay based on the surface plasmon resonance (SPR) biosensor technique was developed to study the interaction between insulin-like growth factor-1 receptor (IGF-1R) and its intracellular substrate protein insulin receptor substrate-1 (IRS-1). The sensor surface was modified with anti-IGF-1R (α-subunit) monoclonal antibodies for the capturing of the receptor-containing membrane fragments from cell lysates. The IGF-1R was successfully immobilized on the sensor surface with binding capability for its intracellular substrates. SPR measurements showed that the tyrosine phosphorylation of IGF-1R induced by its extracellular ligand insulin-like growth factor-1 caused the receptor to bind with IRS-1 10 times faster than the unactivated receptor. As a result, the affinity constants of IRS-1 to phosphorylated and unphosphorylated IGF-1R were $(8.06 \pm 5.18) \times 10^9$ M^{-1} and $(9.81 \pm 4.61) \times 10^8$ M^{-1}, respectively. © **2001 Published by Elsevier Science B.V. on behalf of the Federation of European Biochemical Societies.**

Key words: Insulin-like growth factor-1 receptor; Insulin receptor substrate-1; Tyrosine phosphorylation; Surface plasmon resonance; Biosensor

1. Introduction

The function of insulin-like growth factor-1 (IGF-1) is realized by binding of IGF-1 to insulin-like growth factor-1 receptor (IGF-1R) and inducing their intrinsic tyrosine kinase activity and autophosphorylation. This autophosphorylation of IGF-1R leads to tyrosine phosphorylation of cellular substrates such as insulin receptor substrates and src homology 2/α-collagen. The tyrosine-phosphorylated proteins in turn complex with a variety of src homology 2 (SH2) domain-containing proteins, and initiate specific signal pathways (cf. reviews [1–5]). To date, four members of the insulin receptor substrate (IRS) family, IRS-1 [6,7], IRS-2 [8], IRS-3 [9] and IRS-4 [10], have been identified, as characterized by their similar structure and functions. Each of the IRS proteins consists of an amino-terminal pleckstrin homology domain, a phosphotyrosine binding domain and a large domain containing many motifs for tyrosine phosphorylation and for binding of SH2-containing proteins. IRS-1 was the first to be purified and cloned among the IRS family of proteins [6,7]. A number of studies have investigated the interaction between IGF-1R and IRS-1 in vivo using yeast two hybridization and Western blot techniques [11–17]. However, the effect of receptor autophosphorylation level on the affinity of IRS-1 binding to IGF-1R has not been examined. In addition, quantitative thermodynamic and kinetic profiles of the binding interaction between IRS-1 and IGF-1R with or without ligand activation have not been determined.

Biosensor technology based on the surface plasmon resonance (SPR) technique has been used to measure the binding kinetics between a biomolecule in solution and its binding partner immobilized on a sensor surface in real time [18]. Applications of the SPR biosensor include the study of receptor–ligand interactions, the formation of signaling complexes, epitope mapping and protein–DNA binding [19–23]. SPR biosensor has been used to study the affinities and kinetics of IGF-1 binding with the extracellular fragments of IGF-1R proteins and with its binding proteins [24–27]. Recently an SPR-based method was reported for determination of agonist selectivity of insulin receptor, IRS-1 and its downstream target phosphatidylinositol 3-kinase [28]. This method is based on the competitive binding between two peptide fragments of the signaling molecules in solution and on sensor surface. In a relevant study, an antibody-modified sensor surface was generated and used to capture the epidermal growth factor receptor from cell lysate directly for the binding study of the receptor with its extracellular ligands [29].

Characterization of membrane receptors with their extracellular ligands or intracellular docking proteins/substrates has been limited by the lack of quantitative assays to obtain the kinetic and thermodynamic parameters of these binding interactions. In this study, an in vitro method for detecting IGF-1R and its intracellular substrate IRS-1 interactions based on the SPR biosensor technique was developed. The assay principle is schematically shown in Fig. 1. The IGF-1R (Ab-1) was chemically cross-linked on the sensor chip surface to capture IGF-1R directly from cell lysate containing IGF-1R membrane fractions. Because of the antibody bound specifically to the α-subunit of the receptor, the β-subunit of IGF-1R

*Corresponding author. Fax: (852)-27887406.
E-mail addresses: bhmswong@polyu.edu.hk (M.S. Wong), bhmyang@cityu.edu.hk (M. Yang).

[1] Also corresponding author. Fax: (852)-23649932.

Abbreviations: IGF-1, insulin-like growth factor-1; IGF-1R, insulin-like growth factor-1 receptor; IRS-1, insulin receptor substrate-1; SPR, surface plasmon resonance

0014-5793/01/$20.00 © 2001 Published by Elsevier Science B.V. on behalf of the Federation of European Biochemical Societies.
PII: S0014-5793(01)02780-6

was exposed to the solution phase and available for binding with IRS-1 at the sensor–liquid interface. Each step of the binding assay, including the immobilization of antibody, capturing of the receptor, and binding of IRS-1, could be controlled and monitored by the SPR biosensor in real time. Binding of IRS-1 to the immobilized IGF-1R at different levels of tyrosine phosphorylation can be monitored directly by the SPR biosensor to provide kinetic and thermodynamic information of the interaction.

2. Materials and methods

2.1. Materials

Sensor chips (CM5 research grade), HBS buffer (10 mM HEPES, 150 mM NaCl, 3.4 mM EDTA, 0.05% P20, pH 7.4), and the amine coupling kit containing *N*-hydroxysuccinimide (NHS), *N*-ethyl-*N*′-(3-diethylaminopropyl)carbodiimide (EDC), and ethanolamine hydrochloride were acquired from BIAcore AB (Uppsala, Sweden). IRS-1 was from Upstate Biotechnology Inc. (Lake Placid, NY, USA). Mouse monoclonal antibody against the α-subunit of human IGF-1R [IGF-1R (Ab-1)] was from Calbiochem-Novabiochem Inc. (Cambridge, MA, USA). The IGF-1R (Ab-1) was generated from a fusion FO myeloma cell clone αIR3 and has been shown to preferentially bind to the α-subunit of IGF-1R [30]. Anti-IGF-1R (β-subunit) was purchased from Santa Cruz Biotechnology, Inc. (Santa Cruz, CA, USA). Antibody against phosphotyrosine was obtained from New England Biolabs Inc. (Beverly, MA, USA). Dulbecco's modified Eagle's medium (DMEM), fetal bovine serum (FBS) and a mixture of 10 000 U/ml penicillin and 10 000 μg/ml streptomycin were obtained from Life Technologies Inc. (Grand Island, NY, USA). Geneticin (antibiotic G418) was from Sigma (St. Louis, MO, USA). All other chemicals used were of analytical grade, and doubly distilled deionized water was used in all experiments.

2.2. Cell lines

The NIH-3T3 cell line overexpressing IGF-1R was obtained from Professor Derek LeRoith (National Institute of Diabetes and Digestive and Kidney diseases, NIH, Bethesda, MA, USA). The cells were maintained in DMEM supplemented with 10% FBS, 500 μg/ml G-418, 100 U/ml penicillin, and 100 μg/ml streptomycin. Control NIH-3T3 cell line was maintained in the same medium but without supplementation with G-418. All cell lines were cultured in a humidified atmosphere of 95% air and 5% of CO_2 at 37°C.

2.3. Immunoblotting of receptor autophosphorylation

The cells overexpressing IGF-1R were grown to confluence in 100-mm plates and serum-starved overnight in DMEM without supplementation with FBS. The cells were then incubated either with or without IGF-1 (100 ng/ml) for 1 min at 37°C. IGF-1R and its autophosphorylation were determined by the immunoprecipitation and immunoblotting method previously described [17].

2.4. SPR receptor binding assay

The membrane fraction of the receptor for the SPR assay was prepared based on previously reported protocols [29]. Briefly, the NIH-3T3 cell line overexpressing IGF-1R was grown to confluence in 150-mm plates and incubated either with or without IGF-1 (100 ng/ml) for 1 min at 37°C as described above. The cells were then washed rapidly three times with chilled phosphate-buffered saline and then lysed with 0.6 ml extraction buffer (1% Triton X-100 in 20 mM HEPES, 150 mM NaCl, 1 mM EGTA, pH 7.4, with freshly added phosphatase inhibitor sodium orthovanadate (final concentration 1 mM), and protease inhibitors (final concentration of 0.5 mM phenylmethylsulfonyl fluoride, 1% of protease inhibitors stock solution (100×, 1 M bezaidine, 8% bacitracin, 6 μg/ml aprotinin, 0.2 mM pepstatin, 0.2 mM leupeptin)). The cells were scraped by a cell scraper and collected in a microtube. The plates were then washed by addition of 0.3 ml extraction buffer. The combined lysate was cleared at 4°C by sequential centrifugation at top speed for 15 min (GS-15R centrifuge, Beckman) and at 70 000 rpm for 30 min (NV70 rotor, Beckman). The supernatants containing the membrane fraction of the cell lysate were used in subsequent experiments.

All SPR measurements were performed on the BIAcore™ X apparatus (BIAcore AB, Uppsala, Sweden). The basic principle of the SPR biosensor has been described in detail elsewhere [31–33]. In general, the sensor system probed the refractive index changes in a flow cell due to the binding of molecules to an immobilized ligand. The change in refractive index detected by the sensor was expressed as an arbitrary unit called the resonance unit (RU). The arbitrary resonance units are plotted against time in real time by the BIAcore instrument and the plot is called a sensorgram.

Immobilization of IGF-1R (Ab-1) was carried out by the standard EDC/NHS chemical procedure. Equal volumes of 0.2 M NHS and 0.4 M EDC were mixed just before use and 35 μl of the mixture was injected over the CM5 sensor chip to activate the carboxymethylated dextran hydrogel on the sensor surface. A 35-μl solution of IGF-1R (Ab-1) (20 μg/ml in 10 mM sodium acetate, pH 4.5) was injected over the activated surface, followed by a 35-μl solution of 1 M ethanolamine hydrochloride to deactivate the remaining active carboxyl groups. Immediately after the immobilization, a 15-μl solution of 100 mM HCl was injected three times to remove any remaining non-covalently bound proteins. This was followed by a 3-h wash with HBS buffer. The above immobilization procedure was carried out at 25°C and at a constant flow rate of 5 μl/min using HBS buffer. The antibody-immobilized chip was equilibrated with HBS buffer, followed by the injection of 40 μl of membrane fraction of the lysate to capture IGF-1R from cell lysates. After lysate injection, the sensor chip surface was washed with HPS buffer until a stable baseline was reached. To determine the affinity of IRS-1 to IGF-1R, 32 μl of IRS-1 at different concentrations in HBS buffer (pH 7.4) was injected over the receptor-immobilized sensor chip (association phase), followed by a 10-min wash with HBS buffer (dissociation phase). The sensor surface was then regenerated by one pulse of injection with 4 μl of 10 mM NaOH and 0.5% SDS solution to remove the receptor. The regenerated surface was used for another cycle of receptor capturing and IRS-1 binding experiment. To correct for non-specific binding and bulk refractive index change, a control channel with only the antibody immobilized on the sensor chip surface was used and run simultaneously for each IRS-1 binding experiment. After subtracting the sensorgram from the control channel, the binding of IRS-1 to the captured IGF-1R was obtained. All SPR experiments were carried out at 25°C with a constant flow rate of 8 μl/min in HBS buffer, unless otherwise specified.

2.5. Kinetic models and data analysis

The sensorgrams were analyzed using BIAevaluation™ Software version 3.1. Several binding models including simple one-site, one-site binding with mass transport limit, one-site with conformational change, and two-site binding [34] were used to fit the IRS-1/IGF-1R interaction data using both integrated rate equation and numerical integration methods. The degree of randomness of the residual plot and the reduced $\chi 2$ value were used to assess the appropriateness of a model to the sensor data. The simplest and the most appropriate model for each binding interaction was used to derive the kinetic parameters. In all cases, the one-site model seemed to be sufficient in fitting the data (see Section 3). The respective rate equation can be described as:

$$\frac{d[AB]}{dt} = k_a[A][B] - k_d[AB] \quad (1)$$

where $[AB]$ is the concentration of the bound complex on the sensor surface, $[B]$ is the immobilized binding partner (ligand), $[A]$ is the concentration of the injected binding partner (analyte), and k_a and k_d are the association rate constant and dissociation rate constant, respectively.

Since the response on the sensorgram, R, is directly related to $[AB]$, the rate equation can be integrated to give:

$$\text{For association}: \; R = R_{eq}\{1 - \exp[-(k_a[A] + k_d)(t - t_0)]\} \quad (2)$$

$$\text{For dissociation}: \; R = R_0 \exp[-k_d(t - t_0)] \quad (3)$$

where R_{eq} is the steady-state response level and R_0 is the response at the start of dissociation. It should be noted that the effect of steric interference and re-binding are ignored. The equilibrium affinity constant (K_A) is calculated based on the ratio k_a/k_d. The rate constants may be recovered by fitting the binding curves through non-linear regression analysis of the integrated equations (Eqs. 2 and 3). The mean values of the association rate constants and dissociation rate

constants for the IRS-1 binding to IGF-1R with or without autophosphorylation were obtained from triplicate experiments for each concentration of IRS-1. P values were determined by an unpaired Student's t-test to compare the mean values; $P < 0.1$ was considered to be statistically significant.

3. Results

IGF-1R was captured from the cell lysate directly without the need for purifying the receptor protein. A typical sensorgram for the immobilization of the antibody is shown in Fig. 2. For all experiments, about 1800 RU of immobilized antibody was prepared for all capturing steps. The changes in sensor signal RU correspond to approximately 1.8 ng/mm^2 of antibodies immobilized, based on the estimation that 1000 RU equals 1 ng/mm^2 of surface mass [35]. The captured IGF-1R could not be washed away by HBS buffer but could be completely washed away by the solution containing 10 mM NaOH and 0.5% SDS. The regenerated antibody surface could be reused for subsequent IGF-1R capturing.

The cell lysate containing IGF-1R in the Triton X-100 extract from the transfected mouse NIH-3T3 cell line overexpressing IGF-1R, or the lysate from the control NIH-3T3 cell line, was injected over the antibody-modified sensor chip. It was found that the amount of the captured receptor was completely dependent on the presence of the anti-IGF-1R antibody (Fig. 3). IGF-1R was only captured on the sensor chips modified with the anti-IGF-1R (α-subunit) antibody. The blank CM5 chip surface did not bind IGF-1R. The amount of IGF-1R captured from NIH-3T3 cells overexpressing IGF-1R was significantly greater than that from the control NIH-3T3 cells (600 RU vs. 100 RU). It was reported that the NIH-3T3 cells overexpressing IGF-1R contain about 1×10^6 receptor molecules per cell [17,36]. NIH-3T3 cells overexpressing IGF-1R contained more receptor molecules per cell than NIH-3T3 cell, as confirmed by Western blot experiments (Fig. 4a).

In order to study the effect of IGF-1-induced autophosphorylation of IGF-1R on its binding to IRS-1, the cells overexpressing IGF-1R were treated with overnight serum starvation to eliminate the effect of growth hormones in the culture medium, followed by 100 ng/ml of IGF-1 for 1 min. The IGF-1 treatment induced tyrosine phosphorylation of IGF-1R in its β-subunits, while the untreated cells did not show tyrosine phosphorylation in the β-subunits of IGF-1R (Fig. 4b). In addition, immunoprecipitation detection demonstrated that binding of anti-IGF-1R (α-subunit) antibody to IGF-1R in vitro did not induce the autophosphorylation of IGF-1R.

After capturing IGF-1R from the cell lysate, the sensor surface was washed with HPS buffer for at least 2 h at a flow rate of 8 μl/min until reaching a stable baseline. In all experiments, approximately 380 RU of IGF-1R was captured on the sensor surface for IRS-1 binding. The cell lysate from IGF-1-treated or untreated cells was injected over the antibody-modified sensor surface under identical conditions and similar sensor responses were observed, indicating similar amounts of IGF-1R were captured on the sensor surface. It was shown that IGF-1 stimulation did not affect the binding ability of the α-subunits of IGF-1R with the specific antibody.

The IRS-1 solution at different concentrations was injected over the IGF-1R-modified surface for a period of 240 s, followed by washing with HBS buffer, giving a complete association and dissociation profile of IRS-1 binding with IGF-1R (Fig. 5). After the IRS-1 binding experiment, the surface was regenerated with 4 μl of a 10 mM NaOH/0.5% SDS solution to remove the captured IGF-1R. After 2 h of equilibration with HPS buffer, the baseline returned to the level before capturing IGF-1R. The surface could be used to capture IGF-1R again from the cell lysate and another cycle of IRS-1 binding experiment performed. The antibody-coupling sensor chip could be reused for 30 cycles.

The binding and dissociation of IRS-1 at different concentrations (38.2, 19.1, and 3.64 nM) with the immobilized IGF-1R from IGF-1 activated and unactivated cells are shown in Fig. 5a,b, respectively. With increasing IRS-1 concentration, the SPR signal increases for both activated and unactivated IGF-1R but to different extents. The experiments were repeated three times and the binding data were fitted with var-

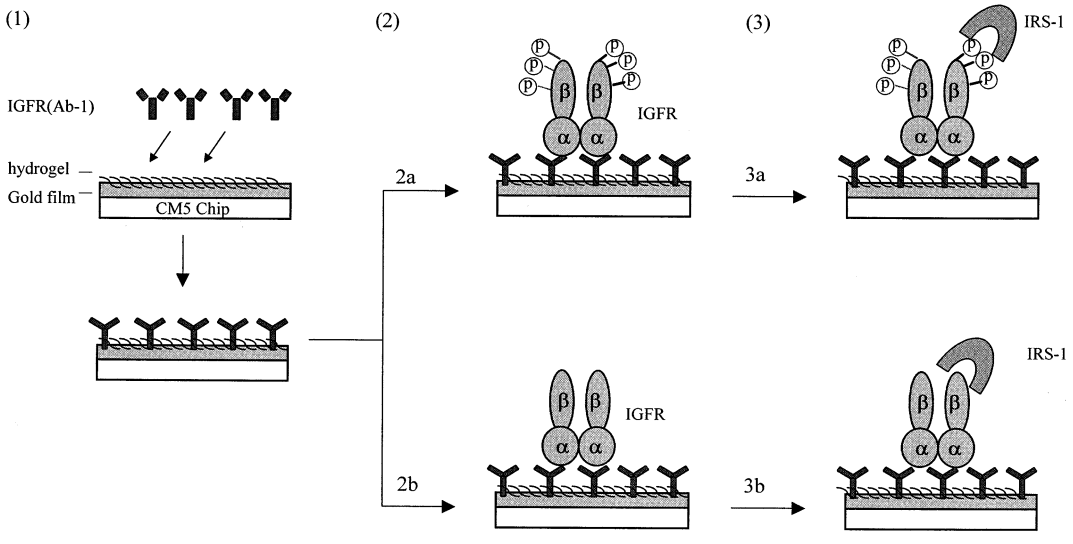

Fig. 1. Principle for the SPR-based receptor binding assay. Step 1, the antibody IGF-1R (Ab-1) is immobilized on the surface of a CM5 chip by standard EDC/NHS reaction. Step 2, the cell lysate obtained from cells incubated with (a) or without (b) 100 ng/ml of IGF-1 is passed through the sensor surface and the IGF-1R is captured by the antibody. The (-p) represents the phosphorylated tyrosine group in the β-subunit of IGF-1R. Step 3, different concentrations of IRS-1 are injected and bind with receptors on the sensor surface.

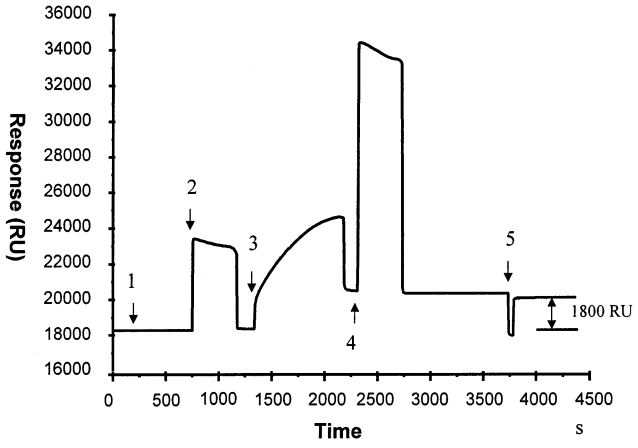

Fig. 2. Real-time sensorgram for IGF-1R (Ab-1) immobilization on SPR sensor surface. The sensor chip (CM5) was equilibrated with HBS buffer (step 1). The carboxylated dextran layer was activated by a solution of NHS and EDC (step 2). 35 μl of 20 μg/ml IGF-1R (Ab-1) in 10 mM acetate buffer, pH 4.5, was then passed over the surface for covalent coupling (step 3), and the residual coupling groups were inactivated by ethanolamine (step 4). The surface was washed by 100 mM HCl (step 5), followed by a 3-h wash with HBS buffer. After the immobilization process, a net increase of 1800 RU in SPR signal was observed which corresponds to a surface density of approximately 1.8 ng/mm^2 covalently bound IGF-1R (Ab-1).

ious kinetic models on both association and dissociation curves simultaneously. The goodness of the fit was judged by the reduced χ^2 values and residual error distributions. The Langmuir binding model was found to be adequate to describe the binding interactions between the receptor and IRS-1. The curve fitting was not significantly improved using more complex models, as judged by the reduced χ^2 values. The fitted k_a and k_d values for each concentration of IRS-1 binding were averaged to give mean values of k_a and k_d for three sets of experiments (Table 1). An unpaired Student's t-test was used to compare the mean values from the two conditions. It was found that IRS-1 binds with IGF-1-activated IGF-1R 10 times faster than with unactivated IGF-1R ($P < 0.1$). The dissociation rate constants of the IRS-1/IGF-1R complexes between the two states of the receptor did not show a significant difference ($P = 0.8$). The affinity constants of IRS-1 to phosphorylated and unphosphorylated IGF-1R were $(8.06 \pm 5.18) \times 10^9$ M^{-1} and $(9.81 \pm 4.61) \times 10^8$ M^{-1} respectively. The affinity of IRS-1 to phosphorylated IGF-1R was 10 times greater than that to unphosphorylated IGF-1R ($P < 0.1$).

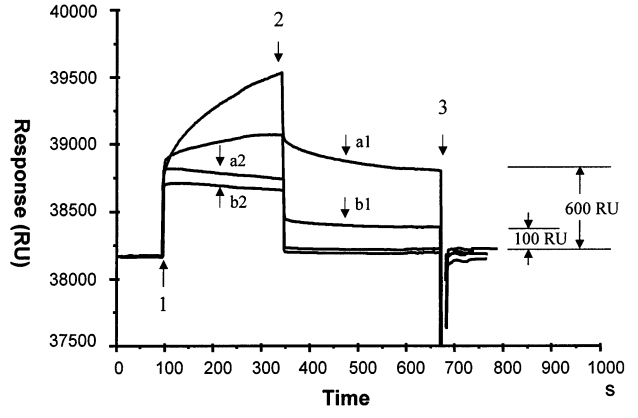

Fig. 3. Sensorgrams for the capturing of IGF-1R from the NIH-3T3 cell line with or without overexpression of IGF-1R by the immobilized anti-IGF-1R antibody. Step 1, injection of cell lysates from the two cell lines over the sensor chip surface. Step 2, washing the sensor chip with HBS buffer. Step 3, regeneration of the sensor chip with a solution containing 10 mM NaOH and 0.5% of SDS. (a1) Injection of cell lysate from the NIH-3T3 cells overexpressing IGF-1R over the sensor chip immobilized with IGF-1R (Ab-1); (b1) injection of cell lysate from the control NIH-3T3 cells over the sensor chip immobilized with IGF-1R (Ab-1); (a2) injection of cell lysate form the NIH-3T3 cells overexpressing IGF-1R over the sensor chip without IGF-1R (Ab-1); (b2) injection of cell lysate from control NIH-3T3 cells over the sensor chip without IGF-1R (Ab-1).

4. Discussion

An SPR-based receptor binding assay was developed that can evaluate the binding characteristics of IRS-1 with IGF-1R with and without IGF-1 stimulation. This is the first time a quantitative kinetic and thermodynamic profile was obtained for the IRS-1/IGF-1R interaction. Our results have confirmed that IGF-1 induces tyrosine phosphorylation of IGF-1R (Fig. 4). IGF-1 binding to the cysteine-rich domain in the extracellular α-subunit of the receptor triggers autophosphorylation of the β-subunits and stimulates the tyrosine kinase activity [17,36]. Each β-subunit then transphosphorylates the other, leading to phosphorylation of a number of tyrosine residues in the carboxy-terminal domain of the β-subunit. Phosphorylation of these residues markedly increases the activity of the kinase domain towards downstream substrates. Our results show that in addition to the increase in IGF-1R kinase activity, the phosphorylated IGF-1R has a higher affinity for its downstream substrate protein IRS-1 than the unphosphorylated IGF-1R (Table 1). Therefore, the tyrosine phosphorylation of IGF-1R has two distinct, but related, outcomes. Firstly, the tyrosine kinase activity of the receptor is enhanced, and secondly, the phosphorylated tyrosine residues

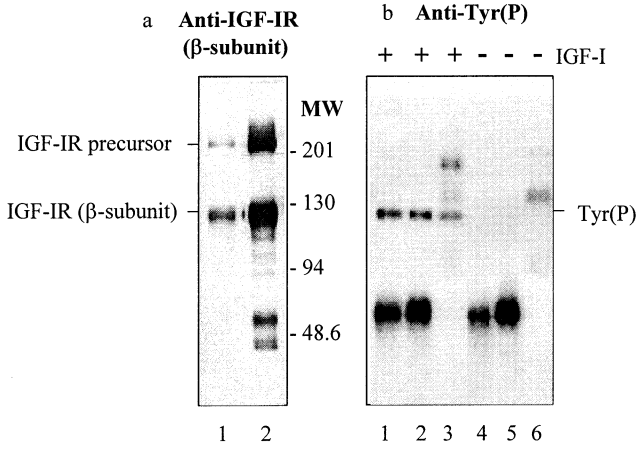

Fig. 4. a: Western blot of IGF-1R (β-subunit) from control NIH-3T3 cells (lane 1) and NIH-3T3 cells overexpressing IGF-1R (lane 2). b: IGF-1 stimulation of IGF-1R autophosphorylation in intact cell. The NIH-3T3 cells overexpressing IGF-1R were stimulated with (+, lanes 1–3) or without (−, lanes 4–6) 100 ng/ml of IGF-1. Lysates (500 μl) were immunoprecipitated with anti-IGF-1R (α-subunit) antibody (lanes 1, 3) or anti-IGF-1R (β-subunit) antibody (lanes 2, 5). Lysates (10 μl) were added in lanes 4 and 6. The tyrosine-phosphorylated proteins (Tyr(P)) were detected by anti-Tyr(P) antibody as described in Section 2.

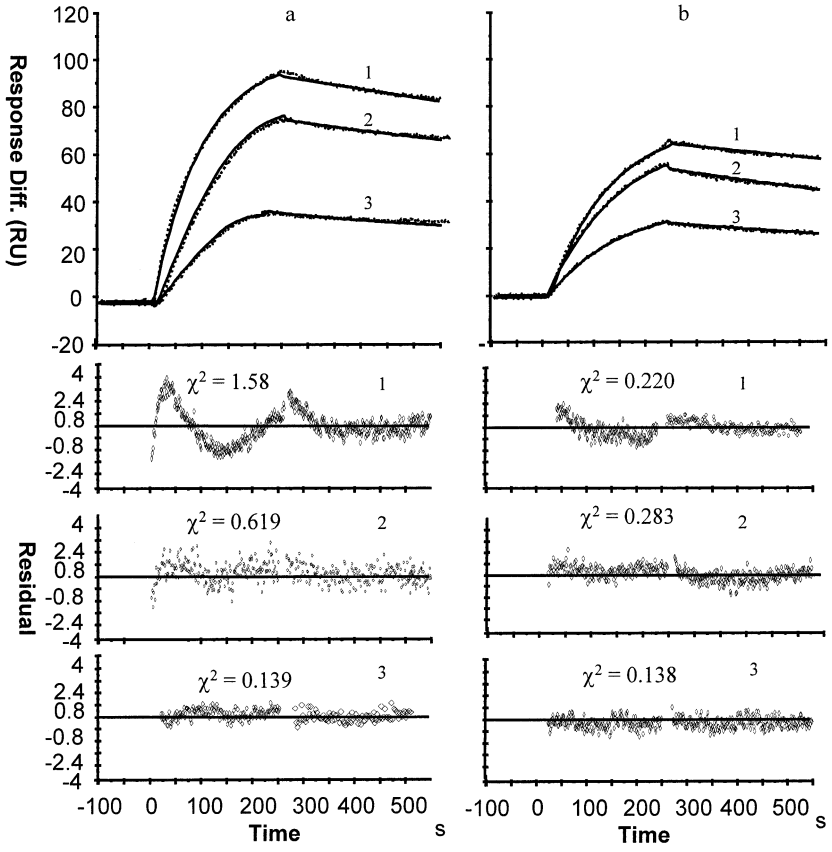

Fig. 5. Sensorgrams showing the binding and dissociation profiles of IRS-1 with the immobilized IGF-1R from the IGF-1R-overexpressing cells incubated in (a) the presence of IGF-1 and (b) the absence of IGF-1. The residual plots of the non-linear regression analysis of the association and the dissociation curves using the one-site binding model (Eqs. 2 and 3) were shown below with the minimum χ^2 values of the fitting. The experimental data (solid lines) and the fitting curves (dotted lines) and the residual plots are shown for three concentrations of IRS-1, (1) 38.2 nM, (2) 19.1 nM, and (3) 3.64 nM, respectively.

provide better binding sites for its substrate proteins that mediate the signaling cascades emanating from the IGF-1 receptor.

Both IGF-1-activated and unactivated IGF-1R showed high affinity towards IRS-1, although the former binds to IRS-1 with one order of magnitude greater affinity. The increase in the affinity constant is mainly due to the increase in the association rate constant of IRS-1 binding to activated IGF-1R. The affinity constant values suggest that the intracellular concentration of IRS-1 should be in the range of 10–100 nM in order for the molecules to respond to the activation of the IGF-1R.

The observed binding affinity of IRS-1 with unactivated IGF-1R in our experiments may be explained by the IGF-1-mimic effect of the antibody αIR-3 we used. It was reported that several monoclonal antibodies against IGF-1R weakly stimulated DNA synthesis in IGF-1R/3T3 cells [37]. This fact has also been demonstrated in mouse NIH-3T3 cells overexpressing human IGF-1R. It is known that αIR-3 is an IGF-1-mimetic antibody that can induce autophosphorylation of the IGF-1R, but the kinetics of autophosphorylation even with a high concentration (100 nM) are slower than those seen with IGF-1 [36]. This effect was observed in intact cells. In our experiments, IGF-1R was associated with αIR-3 on the sensor surface and this binding did not cause autophosphorylation of IGF-1R. In the case of no activation with IGF-1, the receptor may induce a conformational change by αIR-3 on the sensor surface. It is supposed this conformation change may result in an increase of the affinity of receptor binding to IRS-1.

The use of the antibody-capturing approach for receptor–ligand binding study has certain advantages over the direct immobilization method on sensor chip surface. Firstly, specific receptors can be recruited from crude cell lysate without the need for purified proteins. The second benefit is that the receptor can be captured in its membrane state, thus preserving the conformation of the receptor and mimicking the natural environment of the membrane. As a result, the interaction between the captured receptor and the ligand can best mimic the interaction on the cell membrane in vivo. Thirdly, the capturing of the receptor by specific antibody can provide a better control of the orientation of the receptor, exposing the

Table 1
The association and dissociation rate constants and affinity constants for IRS-1 binding to IGF-1R with or without IGF-1 activation

IGF-1R	k_a (M^{-1} s^{-1})	k_d (s^{-1})	K_A (M^{-1})
Activated with IGF-1	$(5.01 \pm 3.35) \times 10^6$	$(6.22 \pm 3.26) \times 10^{-4}$	$(8.06 \pm 5.18) \times 10^9$
Unactivated	$(5.56 \pm 3.66) \times 10^5$	$(5.67 \pm 1.60) \times 10^{-4}$	$(9.81 \pm 4.61) \times 10^8$

fragment of the receptor with its binding site to the solution for ligand binding. This approach can be adopted for studies of the binding between a specific receptor and either its intracellular substrates or its extracellular ligands.

The results obtained in this study clearly demonstrate the feasibility of using the SPR biosensor assay to obtain quantitative information on the kinetics and thermodynamics of the binding interactions between cell membrane receptors and their intracellular and extracellular binding partners.

Acknowledgements: This work was supported by The Research Grants Council of Hong Kong (CityU Project 9040388).

References

[1] LeRoith, D., Werner, H., Beitner-Johnson, D. and Roberts Jr., C.T. (1995) Endocr. Rev. 16, 143–163.
[2] Sepp-Lorenzino, L. (1998) Breast Cancer Res. Treat. 47, 235–253.
[3] LeRoith, D. (2000) Endocrinology 141, 1287–1288.
[4] Sasaoka, T., Rose, D.W., Jhun, B.H., Saltiel, A.R., Draznin, B. and Olefsky, J.M. (1994) J. Biol. Chem. 269, 13689–13694.
[5] Myers Jr., M.G., Sun, X.J. and White, M.F. (1994) Trends Biochem. Sci. 19, 289–293.
[6] White, M.F., Maron, R. and Kahn, C.R. (1985) Nature 318, 183–186.
[7] Sun, X.J., Rothenberg, P., Kahn, C.R., Backer, J.M., Araki, E., Wilden, P.A., Cahill, D.A., Goldstein, B.J. and White, M.F. (1991) Nature 352, 73–77.
[8] Sun, X.J., Wang, L.M., Zhang, Y., Yenush, L., Myers Jr., M.G., Glasheen, E., Lane, W.S., Pierce, J.H. and White, M.F. (1995) Nature 377, 173–177.
[9] Lavan, B.E., Lane, W.S. and Lienhard, G.E. (1997) J. Biol. Chem. 272, 11439–11443.
[10] Lavan, B.E., Fantin, V.R., Chang, E.T., Lane, W.S., Keller, S.R. and Lienhard, G.E. (1997) J. Biol. Chem. 272, 21403–21407.
[11] Craparo, A., O'Neill, T.J. and Gustafson, T.A. (1995) J. Biol. Chem. 270, 15639–15643.
[12] He, W., Craparo, A., Zhu, Y., O'Neill, T.J., Wang, L.M., Pierce, J.H. and Gustafson, T.A. (1996) J. Biol. Chem. 271, 11641–11645.
[13] Sawka-Verhelle, D., Tartare-Deckert, S., White, M.F. and Van Obberghen, E. (1996) J. Biol. Chem. 271, 5980–5983.
[14] Tartare-Deckert, S., Sawka-Verhelle, D., Murdaca, J. and Van Obberghen, E. (1995) J. Biol. Chem. 270, 23456–23460.
[15] Dey, B.R., Frick, K., Lopaczynski, W., Nissley, S.P. and Furlanetto, R.W. (1996) Mol. Endocrinol. 10, 631–641.
[16] Rocchi, S., Tartare-Deckert, S., Sawka-Verhelle, D., Gamha, A. and van Obberghen, E. (1996) Endocrinology 137, 4944–4952.
[17] Hernandez-Sanchez, C., Blakesley, V., Kalebic, T., Helman, L. and LeRoith, D. (1995) J. Biol. Chem. 270, 29176–29181.
[18] Malmqvist, M. (1993) Nature 361, 186–187.
[19] Brigham-Burke, M., Edwards, J.R. and O'Shannessy, D.J. (1992) Anal. Biochem. 205, 125–131.
[20] End, P., Gout, I., Fry, M.J., Panayotou, G., Dhand, R., Yonezawa, K., Kasuga, M. and Waterfield, M.D. (1993) J. Biol. Chem. 268, 10066–10075.
[21] Fägerstam, L.G., Frostell, Å., Karlsson, R., Kullman, M., Malmqvist, A. and Butt, H. (1990) J. Mol. Recogn. 3, 208–214.
[22] Bondeson, K., Frostell, Å., Fägerstam, L.G. and Mgnusson, G. (1993) Anal. Biochem. 214, 245–251.
[23] Dubs, M.-C., Altschuh, D. and Van Regenmortel, M.H.V. (1991) Immunol. Lett. 31, 59–64.
[24] Jansson, M., Uhlen, M. and Nilsson, B. (1997) Biochemistry 36, 4108–4117.
[25] Jansson, M., Dixelius, J., Uhlen, M. and Nilsson, B.O. (1997) FEBS Lett. 416, 259–264.
[26] Jansson, M., Hallen, D., Koho, H., Andersson, G., Berghard, L., Heidrich, J., Nyberg, E., Uhlen, M., Kordel, J. and Nilsson, B. (1997) J. Biol. Chem. 272, 8189–8197.
[27] Wong, M.S., Fong, C.C. and Yang, M. (1999) Biochim. Biophys. Acta 1432 (2), 293–301.
[28] Yoshida, T., Sato, M., Ozawa, T. and Umezawa, Y. (2000) Anal. Chem. 72, 6–11.
[29] Boll, W., Gallusser, A. and Kirchhausen, T. (1995) Curr. Biol. 5, 1168–1178.
[30] Kull Jr., F.C., Jacobs, S., Su, Y.F., Svoboda, M.E., Van Wyk, J.J. and Cuatrecasas, P. (1983) J. Biol. Chem. 258, 6561–6566.
[31] Jönsson, U. and Malmquvist, M. (1992) Adv. Biosensors 2, 291–336.
[32] Fägerstam, L.G. and Karlsson, R. (1993) in: Immunochemistry (van Oss, C.J. and Van Regenmortel, M.H.V., Eds.), pp. 949–970, Marcel Dekker, New York.
[33] BIAapplications Handbook (1994) Pharmacia Biosensor AB, Uppsala.
[34] Karlsson, R. (1994) Anal. Biochem. 221, 142–151.
[35] Stenberg, E., Persson, B., Ross, H. and Urbaniczky, C. (1991) J. Colloid Interface Sci. 143, 513–526.
[36] Hisanori, K., Faria, T.N., Stannard, B., Roberts Jr., C.T. and LeRoith, D. (1993) J. Biol. Chem. 268, 2655–2661.
[37] Soos, M.A., Field, C.E., Lammers, R., Ullrich, A., Zhang, B., Roth, R.A., Andersen, A.S., Kjeldsen, T. and Siddle, K. (1992) J. Biol. Chem. 267, 12955–12963.